JOURNAL OF MATERIALS SCIENCE 29 (1994) 504–509

# Laser cladding and alloying of a Ni-base superalloy on plain carbon steel

S. TOSTO, F. PIERDOMINICI
*Enea Casaccia, via Anguillarese 301, 00060 Roma, Italy*
M. BIANCO
*RTM, 10080 Vico Canavese (To), Italy*

This paper shows that the laser cladding and alloying of a Ni-base superalloy on a substrate of plain carbon steel can be successfully carried out by irradiating a bilayer sample formed by metallic sheets mechanically clamped together. Under laser irradiation, both the overlayer and the substrate are locally melted. Controlled dilution of the alloy elements of the superalloy in the melted pool allows a variety of surface chemical compositions and microstructures to be obtained.

## 1. Introduction

It is known that the surface chemical composition and microstructure of materials can be modified by-high energy beam irradiation [1]. Laser- and electron-beam treatments are examples of advanced processing which enable improvement of the corrosion [2], wear [3] and fatigue-resistance [4] properties of materials. Previous research has shown that the cladding and alloying of the substrates of mild steels [5], stainless steels [6] and Al alloys [7] can be successfully carried out by electron-beam irradiation; the samples were formed by an overlayer sheet (Ni, Ti or Ti alloys, stainless steel) mechanically clamped on the substrate. The treatment parameters were optimized to melt the overlayer and a controlled amount of the substrate, thus leading to a variety of surface chemical compositions and microstructures. Electron microscopy, microprobe analysis, Mössbauer spectroscopy and X-ray diffraction (XRD) have demonstrated that by treating a bilayer (AISI 316 stainless steel/mild steel) a variety of surface steels can be obtained, depending on the treatment conditions and the initial thickness of the overlayer [8]; the chemical compositions after solidification of the molten pool ranged from a composition which was practically identical to that of the original AISI to a composition where the alloy elements were diluted by a factor of about five during the melting process. Austentic, bainitic, martensitic and "duplex" microstructures were consequently obtained [9]; also values of the surface microhardness were found ranging from that of the untreated austenitic stainless steel to values typical of a tempered martensite. The corrosion behaviour of the irradiated samples was found to be in agreement with the observed microstructures [10, 11]. Analogous results were also obtained with the other bilayers mentioned above, thus showing that the thermal contact between the overlayer and the substrate under the given experimental conditions effectively enabled a controlled melting process followed by a predictable modification of both the surface chemical composition and the microstructure. It is suggested that such an experimental procedure could be repeated with a $CO_2$ laser beam. This seems reasonable because the three main phenomena enabling successful cladding or alloying process (namely, (i) surface melting, (ii) element diffusion at the liquid–solid interface, and (iii) convection-driven flow of matter under temperature gradients) are essentially the same in both cases. Then, an experimental procedure similar to that described above was carried out to investigate the possibility of alloying or cladding, by laser irradiation, a Ni-base superalloy sheet clamped on a substrate of plain carbon steel. The purpose of the present paper is to show the possibility of controlling the irradiation conditions in order to obtain surfaces with chemical compositions ranging from those of the original superalloy to those of low alloyed steels.

## 2. Experimental procedure

A rectangular sheet of superalloy with dimensions of $8 \times 50 \times 0.9$ mm$^3$ (width, length and thickness, respectively) was superimposed and fixed by means of some laser-welding spots on a substrate of a low alloyed steel 9 mm thick and 4 cm wide. The chemical compositions of the substrate and superalloy are reported in Table I; the respective microstructures are shown in Fig. 1a and b. A beam integrator was used to obtain a $10 \times 10$ mm$^2$ laser spot. Seven samples were irradiated under different processing parameters; the experimental irradiation conditions are reported in Table II. Cross-sections of the irradiated samples were polished and etched by the usual metallographic procedures; observations were then carried out by scanning electron microscopy (SEM). Concentration profiles of Fe, Cr and Ni, the main alloy elements characterizing both the overlayer and the substrate, were obtained by


0022–2461 

TABLE I Chemical compositions (wt %) of the (a) Mild steel substrate, and (b) the Ni-base superalloy

(a)

| C | Mn | Cr | Cu | Ti | Al | Si | S | P | Fe |
|---|---|---|---|---|---|---|---|---|---|
| 0.14 | 1 | 0.8 | < 0.4 | < 0.01 | 0.015 | 0.1 | 0.025 | < 0.04 | Balance |

(b)

| Ni | Cr | Fe | Ti |
|---|---|---|---|
| 70.93 | 16.83 | 8.64 | 2.86 |

TABLE II Laser-treatment conditions

| Sample | Power (kW) | Travel speed (m min$^{-1}$) | Interaction time (s) |
|---|---|---|---|
| 1 | 8 | 0.4 | 1.5 |
| 2 | 7 | 0.4 | 1.5 |
| 3 | 10 | 0.5 | 1.2 |
| 4 | 7 | 0.25 | 2.4 |
| 5 | 7 | 0.5 | 1.2 |
| 6 | 9 | 0.5 | 1.2 |
| 7 | 10 | 0.25 | 2.4 |

energy dispersive microanalysis to investigate the effects of laser irradiation on the composition of the samples near the surface and at the interface with the substrate. These concentration profiles were taken in correspondence to the bead centreline, perpendicularly to the surface. The depth of the chemically affected zone ranged from about 1 to 3 mm, depending on the treatment parameters. No cracks nor porosities were observed in any of the examined samples. The micrographs in Figs 2, 3 and 4 show the microstructures of samples 3, 6 and 4 of Table II at the interface with the substrate; Figs 5 and 6 show the microstructures of samples 4 and 6 in the bulk of the melted zones. These micrographs demonstrate that, as expected, different

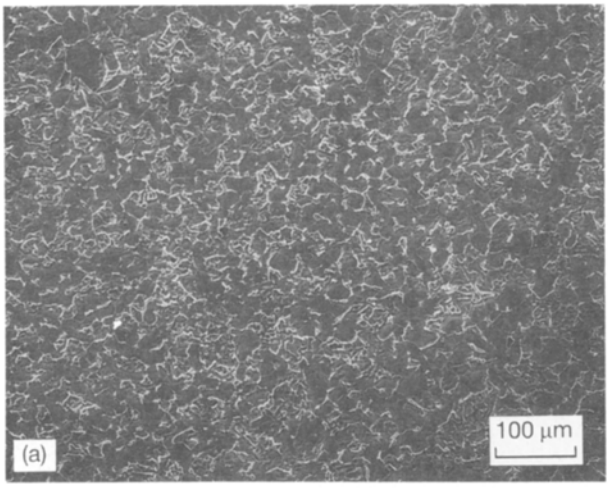


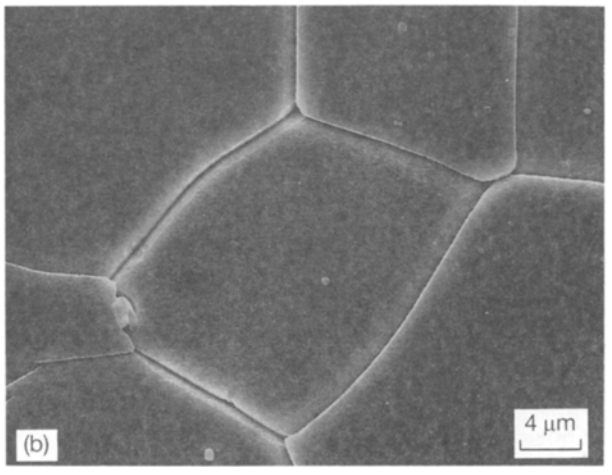


*Figure 1* Microstructures of: (a) the mild steel used as a substrate, and (b) the superalloy used as an overlayer.

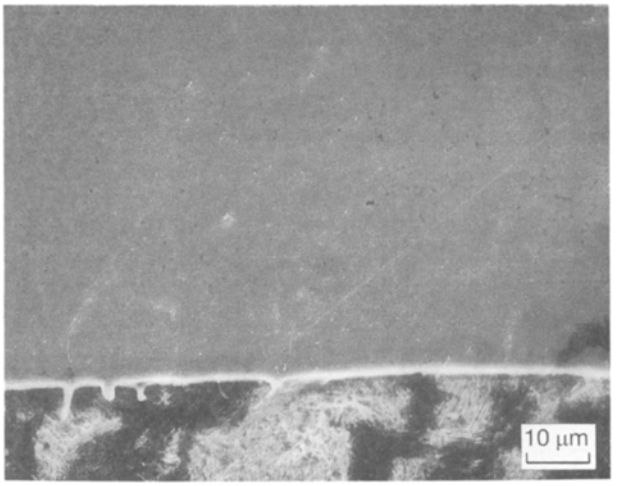


*Figure 2* Microstructure at the interface of sample 3.

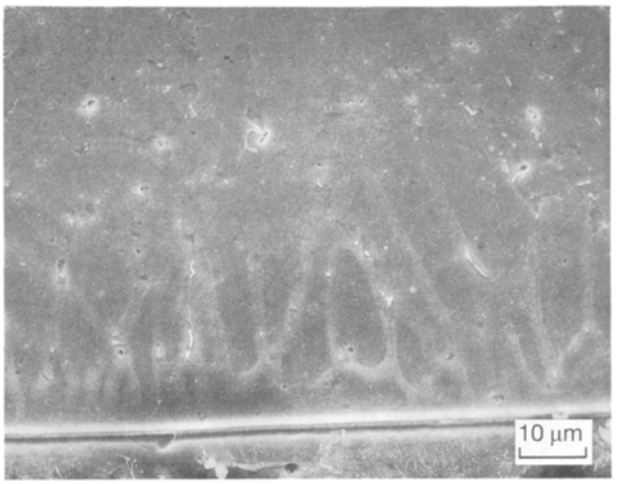


*Figure 3* Microstructure at the interface of sample 6.

microstructures and interface morphologies are obtained under the various treatment conditions. Three examples of trends in the examined elements, as a function of depth across the boundary of the molten pool, are given in Figs 7 to 9.

## 3. Discussion

Steady concentration profiles of Fe, Ni and Cr were found in the bulk of the molten zone of all the treated samples; the typical trends of diffusion profiles were only evidence in the interface near the substrate.

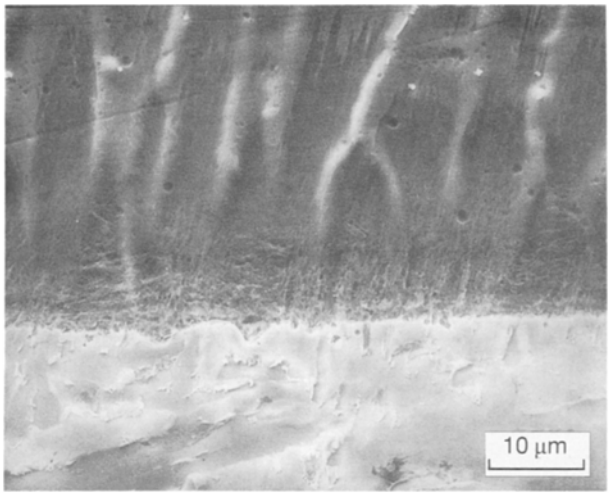


*Figure 4* Microstructure at the interface of sample 4.

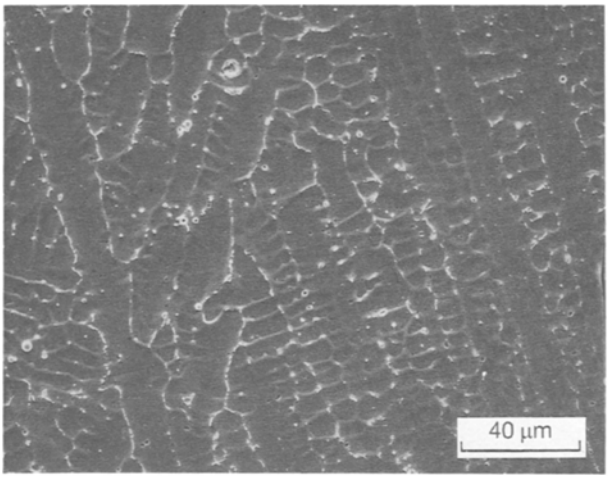


*Figure 5* Microstructure of the melted zone of sample 4.

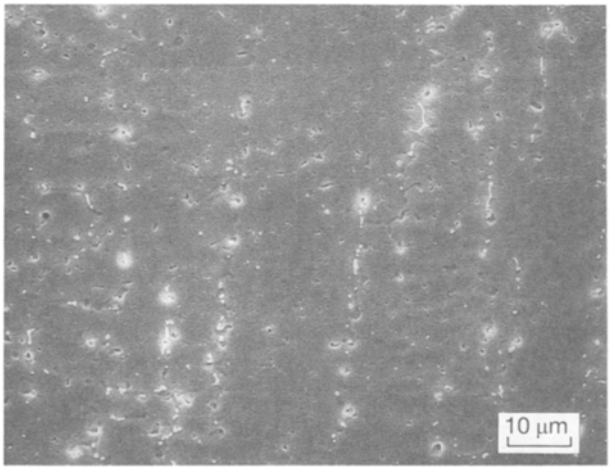


*Figure 6* Microstructure of the melted zone of sample 6.

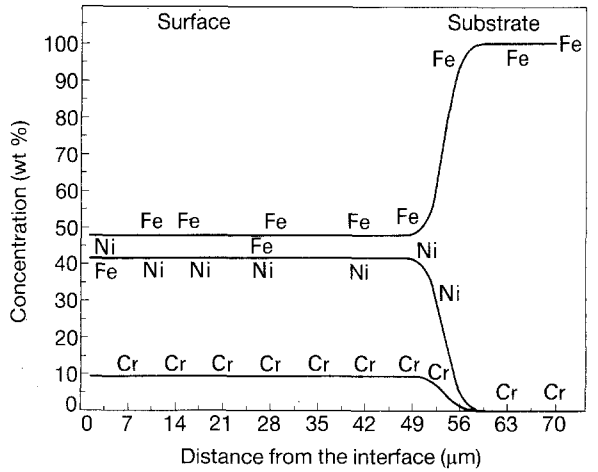


*Figure 7* Calculated concentration profiles of Ni, Cr and Fe near to the interface of sample 1. The symbols of the elements indicate the experimental concentrations of the respective elements obtained by energy dispersive microanalysis.

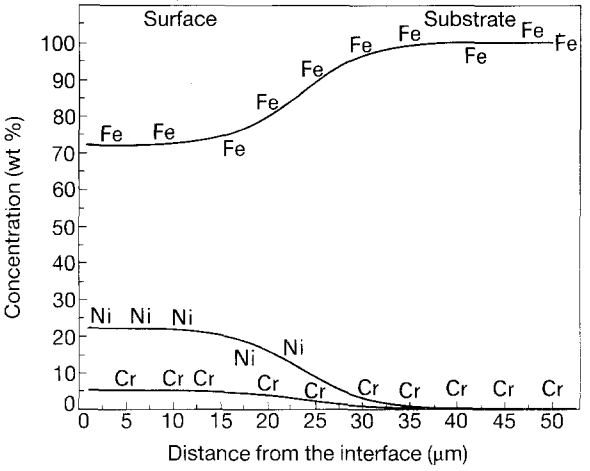


*Figure 8* As for Fig. 7 but for sample 4.

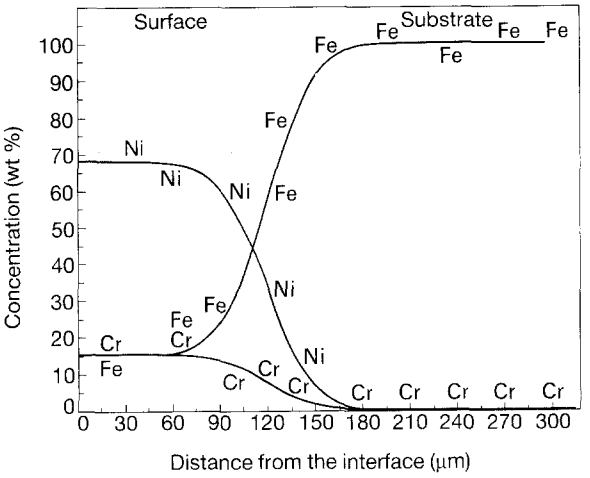


*Figure 9* As for Fig. 7 but for sample 5.

Therefore, a well-defined chemical composition can be related to each treatment condition; this allows definition of the processing parameters enabling cladding or alloying. The microprobe analysis shows that the percentage content of Ni, Cr and Fe after solidification of the molten pool ranges from values that are very similar to those of the untreated superalloy to values which are about six times lower. Therefore, a cladded superalloy or low alloyed surface steels were obtained after laser irradiation in the experimental conditions described above. The main phenomena affecting the final composition of the laser-treated

zone are: (i) the dilution of the elements of the overlayer sheet in the molten pool, and (ii) the diffusion of elements from or towards the substrate at the liquid–solid interface during melting. The dilution factor of a given element of the superalloy is defined as $C_{act}/C_{sup}$, that is, as the ratio of the actual concentration in the alloyed or cladded layer to the concentration of the untreated superalloy; this can be approximated by the ratio $R/(\Delta + R) = 1/(\delta + 1)$, where $\Delta$ is the thickness of the substrate melted together with the superalloy, $R$ is the initial thickness of the superalloy sheet, and $\delta = \Delta/R$. In effect, the surface concentrations found by microanalysis agree with those calculated by the total melt depth, $R + \Delta$. Then, if $\delta \ll 1$, the composition of the molten pool after solidification is expected to be very similar to that of the unaffected superalloy; cladding is thus obtained. For obvious reasons, values of $\delta \gg 1$ are typical of an alloying process. The values of $\Delta$, reported in Table III, range from 0.08 to 2.5; this confirms, in agreement with the microanalysis data, that both cladding and alloying can be obtained – depending on the respective processing conditions: samples 3 and 5 of Table III, characterized by small values of $\delta$, identify cladding treatments; samples 4 and 7 are examples of alloying treatments. Two sets of irradiation conditions can be recognized in Table III: (i) those with the same beam power and different interaction times, and (ii) those with the same interaction time and different beam powers. It is easy to recognize that the interaction time $\tau$, of the laser beam plays a major role in the value of $\delta$. When $\tau$ doubles $\delta$ increases by a factor about 30 at 7 kW (samples 4, 2 and 5 of Table III) and by a factor of 25 at 10 kW (samples 7 and 3). In contrast, the dependence of $\delta$ on the irradiation power, the interaction time being the same, is weaker. Samples 4 and 7, treated with $\tau = 2.4$ s, show that 6 changes from 2.56 to 2.78, when the beam power increases from 7 to 10 kW. Samples 5, 6 and 3, treated with $\tau = 1.2$ s, show that $\delta$ changes from 0.09 to 0.5, i.e. less than 6 times, with the same increase of power. Then the interaction time affects the position of the liquid–solid interface more than the beam power.

More refined statistical calculations are not possible because of the limited number of samples; however, the above figures show that the transition from cladding to alloying is more effectively obtained by increasing the interaction time rather than the beam power. However, $\delta$ alone is not sufficient, in principle, to completely characterize the final composition of the solidified molten pool. This fact has been already evidenced by irradiating, with an electron beam, a sheet of AISI 316 (containing 0.025 wt % C) on a substrate of C40 mild steel (0.4 wt % C) [8]. Line-profile analysis of XRD peaks and observation of the morphology of the phases formed after irradiation were carried out on the alloyed surfaces of the samples: both the broadening of the $\alpha$-ferrite peak and the formation of lath martensite, typical of low–medium alloyed steels, can be explained by hypothesizing the diffusion of C from the substrate towards the molten pool. A way of quantifying this point has been already been discussed in a previous paper [5], which introduced the concept of diffusion length. This was derived by assuming the validity of Fick's diffusion law in the case of a liquid–solid interface at the boundary of the molten pool, and expressing the solution of the diffusion equation as a function of a parameter $L$ called the diffusion length. Clearly, $L$ replaces the well-known quantity $2(Dt)^{1/2}$, $D$ being the diffusion coefficient and $t$ the time elapsed for the diffusion process. $L$ takes into account that the liquid–solid interface is really a layer of finite thickness, known as the mushy zone [12], formed by a mixture of solid and liquid phases; it has simply a phenomenological meaning, summarizing the tendency of the elements to move across the interface, from and towards the substrate. In fact, it was calculated in [5] as a best-fitting parameter to match the solution of Fick's equation with the experimental values of the element concentrations as a function of depth. The agreement between experimental and calculated diffusion profiles was found to be very good for all the treatment conditions, and this showed that Fick's law is adequate to describe the diffusion at the interface. The question arises as to whether or not such a way of calculating the diffusion profiles also holds in the present case. For this reason, a one-dimensional model was used to evaluate the possible contribution of the diffusion-driven element exchange between the substrate and the overlayer to the final composition of the molten pool. Also, in the present case, Fick's law was assumed as a valid way of describing the diffusion. The one-dimensional approximation is legitimate because the thickness of the diffusion layer is of the order of magnitude of few tens to a few hundreds of micrometers (Figs 7 to 9) while the width of the molten pool is of the order of centimetres. The following discussion shows that the experimental diffusion profiles of Fe, Ni and Cr can be fitted using a solution of Fick's equation as a function of the steady element concentration far from the interface, that is, in the bulk of the molten zone. First, high diffusion coefficients are expected at the liquid–solid interface. In fact, interaction times of the order of 1 s enable concentration profiles to be obtained of Ni, Cr and Fe which are similar to those obtained after hours of treatment at a constant temperature in the usual solid–solid diffusion processes. This can be better evidenced as follows. Let $R$ be the initial thickness of superalloy overlayer and $S$ be that of the mild-steel substrate $S$; $C_i(x, t)$ is the

TABLE III Processing parameters. $\Delta$ is the thickness of the molten substrate, $\delta = \Delta/R$ and $L$ is the diffusion length of Fe, Ni and Cr

| Sample | $\tau$ (s) | Power (kW) | $\Delta$ (mm) | $\delta$ | $L$ ($\mu$m) | $\lambda$ $\times 10^3$ | $\xi$ $\times 10^3$ |
|---|---|---|---|---|---|---|---|
| 1 | 1.5 | 8 | 0.75 | 0.83 | 11 | 6.6 | 15 |
| 2 | 1.5 | 7 | 0.6 | 0.67 | 15 | 10.0 | 25 |
| 3 | 1.2 | 10 | 0.1 | 0.11 | 13 | 13.0 | 130 |
| 4 | 2.4 | 7 | 2.3 | 2.56 | 50 | 15.6 | 22 |
| 5 | 1.2 | 7 | 0.08 | 0.09 | 34 | 34.7 | 425 |
| 6 | 1.2 | 9 | 0.45 | 0.5 | 67 | 68.3 | 149 |
| 7 | 2.4 | 10 | 2.5 | 2.78 | 50 | 14.7 | 20 |

concentration of the $i$th element as a function of the co-ordinate $x$ at the time $t$. The boundary conditions of the problem are then

$$C_i(x, 0) = C_r \ (x \leq R), \ C_i(x, 0) = C_s \ (x > R) \tag{1}$$

where the symbols $C_r$ and $C_s$ indicate the initial concentrations of the $i$th element in the overlayer and the substrate, respectively. Moreover, $C_i(x, t)$ must be such that

$$C_i(x, \infty) = \text{const} = \frac{RC_r + SC_s}{R + S} \tag{2}$$

Equation 2 describes, in the one-dimensional approximation, the complete dilution of the $i$th element in a total thickness $R + S$ for $t$ tending to infinity. If the diffusion coefficient, $D$, is assumed to be independent of concentration at constant temperature, then the solution of Fick's equation in the case of a solid–solid diffusion process is

$$C_i(x, t) = \frac{RC_r + SC_s}{R + S} + 0.5(C_r - C_s) \times \left\{ \text{erf}\left[\frac{x}{2(Dt)^{1/2}}\right]\frac{S - R}{S + R} - \text{erf}\left[\frac{x - R}{2(Dt)^{1/2}}\right]\right\} \tag{3}$$

where erf denotes the error function. It can be immediately verified that Equation 3 fullfils the boundary conditions of Equations 1 and 2. In the case of diffusion at the boundary of the laser-induced liquid pool it is necessary to take into account that a suitable amount of substrate is melted together with the overlayer; then, the diffusing layer is the total melt depth $R + \Delta$, where $\Delta$ is the thickness of the substrate involved in the melting process together with the overlayer sheet. Of course, the thickness of the solid substrate is now $S - \Delta$. Equation 3 then becomes

$$C_i(x, t) = \frac{RC_r^* + SC_s}{R + S} + 0.5(C_r^* - C_s) \times \left\{ \text{erf}\left[\frac{x}{L}\right]\frac{S - R - 2\Delta}{S + R} - \text{erf}\left[\frac{x - R - \Delta}{L}\right]\right\} \tag{4}$$

where $L = 2(D^*t)^{1/2}$. The asterisks label the element concentrations corrected for the dilution in the molten pool.

In the above equation, the thickness of the liquid phase, $R + \Delta$, plays the role of the overlayer $R$ in Equation 3. Accordingly, $C_r$ has been replaced by $C_r^*$, which accounts for the dilution in the molten pool of the $i$th element when a thickness, $\Delta$, of the substrate is also melted

$$C_r^* = \frac{C_r R}{R + \Delta} \tag{5}$$

It is clear that $D^*$, appearing in Equation 4 via $L$, is conceptually different from $D$ in Equation 3: $D$ has a well-known meaning [13] and can be taken from the literature data; $D^*$ refers to a completely different experimental situation.

Equations 4 and 5 can be calculated once $\Delta$ and $D^*t$ are known. The former can be inferred from experimental observation of the melt thickness. The latter can be easily found as a best-fitting parameter in Equation 4 to match the experimental concentration profiles. Of course, the best-fit procedure has a meaning only if the results themselves demonstrate the validity of Equation 4 from a physical point of view. In effect, the concentrations of Ni, Fe and Cr calculated with the values of $L = 2(D^*t)^{1/2}$ reported in Table III agree very well in all cases with the experimental results; Figs 7 and 9 are three examples of this, and they show that Fick's equation adequately describes the diffusion of the elements concerned at the liquid–solid interface. Once $D^*t$ is known, $D^*$ can also be calculated as a function of the time, $t$, allowed for the diffusion to occur. This requires an exact knowledge of the length of the melting process, thus accurate modelling is needed of the beam–solid interactions in the given experimental conditions. However, the order of magnitude expected for $D^*$ can be easily evaluated using the interaction time, $\tau$. It is clear from both Equations 3 and 4 that $2(Dt)^{1/2}$ is a reference length determining the scale of the diffusion-affected zone and also the thickness where a significant change of composition is expected; in effect, the graphs in Figs 7 to 9 show that the values of $2(D^*t)^{1/2}$ ( $= L$) reported in Table III are comparable with the respective widths of the diffusion zone. The latter then has an order of magnitude of some tens to hundreds of micrometres, depending on the treatment parameters. Therefore $D^*$ ranges between values of the order of $10^{-7}$ to $10^{-5}$ $cm^2 s^{-1}$. As expected, the laser-induced diffusion at the mushy zone can be simulated with very high diffusion coefficients. More complicated calculations to evaluate $D^*$ have been omitted because, for the purposes of the present paper, the diffusion length $2(D^*t)^{1/2}$ is more important than the value of $D^*$ itself. This can be realized examining the following ratios: $\lambda = 2(D^*t)^{1/2}/(R + \Delta)$ and $\xi = 2(D^*t)^{1/2}/\Delta$. The meaning of these quantities is easily understood.

1. $\lambda$ compares the scale of the diffusion zone, where the concentration of the $i$th element is significantly affected, with the initial thickness of overlayer. Then, $\lambda$ describes the involvement of the molten phase in the diffusion process. Clearly, $\lambda \ll 1$ means that in the given experimental irradiation conditions the scale of the diffusion zone does not involve a significant amount of the liquid phase; on the contrary, higher values of $\lambda$ mean that diffusion is increasingly important in changing, together with the dilution, the chemical composition of the laser-melted zone.

2. The irradiation conditions certainly affect both the total melt depth and the diffusion rate at the liquid–solid interface. In this respect, it is possible to ask whether a higher power or interaction time preferentially increase either the displacement of the interface to higher depths or the tendency of the elements of the molten pool to diffuse. The meaning of $\xi$ is thus clear: it compares the rate with which the elements diffuse across the interface to the rate with which the

interface moves towards the substrate. The values of $\lambda$ and $\xi$ are shown in Table III.

Even without a detailed statistical analysis of the data, the following information can be inferred by simply examining the experimental results in Table III.

1. At a constant interaction time, $\xi$ is a decreasing function of the beam power. This is shown by samples 4 and 7 ($\tau = 2.4$ s), 2 and 1 ($\tau = 1.5$ s), and 5, 6 and 3 ($\tau = 1.2$ s). This suggests that in this case, the predominant effect of a higher beam power is to increase the melt depth rather than the mobility of the atoms at the interface. The same set of samples shows that the trend in $\lambda$ is not clearly evident; it suggests that the irradiation power affects mainly the melt depth.
2. At a constant beam power, $\xi$ decreases with the interaction time; this can be inferred from samples 4, 2 and 5 (7 kW), and 7 and 3 (10 kW). Then, the displacement of the interface increases as a function of $\tau$ more rapidly than the diffusion length. Also, in this case, the dependence of $\lambda$ on $\tau$ is not clearly evident.

In conclusion, the experimental results suggest that at high powers and interaction times of the laser beam the depth of the interface is affected more than the tendency of Fe, Ni and Cr to diffuse. Therefore, the surface composition is essentially controlled by the dilution of the alloy elements of the overlayer in the molten pool when the irradiation energy is increased. These conclusions help to optimize the most convenient choice of processing parameters depending on whether the result expected is cladding or alloying.

Finally, it is worth noting that the values of the diffusion length of Ni, Fe and Cr are the same for each treatment condition; for this reason, a unique value of $L$ has been reported in Table III. Then, the same diffusion coefficient would be calculated, for each treatment condition, through the respective values of $2(D^*t)^{1/2}$. This could not be expected from the well-known mechanisms of atomic jumps between the lattice sites of ordinary diffusion processes [14]. Nevertheless, this experimental result appears reasonable. In fact, the liquid–solid interface is really a layer of finite thickness rather than a plane separating two phases. Then the idea of single atoms leaving the liquid phase to diffuse within a solid lattice is unrealistic. This suggests the hypothesis that the liquid phase itself diffuses within the mushy zone; accordingly, the concentration gradients are due to the mixing of different amounts of liquid and solid phases (with a progressive increase of the latter when approaching the unmelted substrate), rather than to the displacement of single atoms. Accordingly, the microstructure at the interface should be the result of a local mixing between melted and unmelted phases. Such a hypothesis can be confirmed with a more detailed analysis of the interface microstructures; this is in progress at present.

## 4. Conclusion

The experimental results show that the laser irradiation of bilayer samples allows optimization of the melting conditions and the diffusion mechanisms at the liquid–solid interface to obtain cladding or alloying. Accordingly, different final microstructures are obtained. The experimental concentration profiles of Fe, Ni and Cr can be fitted with a Fick-diffusion model. The results of the treatments are predictable in accordance with pre-defined requirements. It is possible, in fact, to define the processing conditions as a function of a given final chemical composition of the molten pool. It allows to control also the composition of the cladded or alloyed zone obtained after solidification. This shows that the experimental procedure described can be successfully used not only to investigate the surface microstructures related to the treatment parameters but also for possible technological applications.

## Acknowledgement

This research was carried out with the financial support of the European Community under BRITE Project P2357.

## References

1. C. W. DRAPER and J. M. POATE *Int. Metal Rev.* **30**(2) (1985) p. 85.
2. E. LUGHEIDER, B. C. OBERLANDER and H. MEINHARDT, in Proceedings of the Third European Conference on Laser Treatment of Materials, edited by H. W. Bergmann and R. Kupfer, (Sprechsaal, Coburg, Germany, 1990).
3. J. D. AYERS, R. J. SCHAEFER and W. P. ROBEY, *J. Metals* August (1981) p. 19.
4. B. L. MORDIKE, in "Laser surface treatment of metals", edited by C. W. Draper and P. Mazzoldi, NATO, ASI Series, Series E: Applied Science (Martinus Nijhoff, Boston, 1986).
5. S. TOSTO and F. NENCI, Memoires et Etudes Scientifiques, Revue de Metallurgie, June 1987, pp. 311, 320.
6. C. VIGNAUD, M. KEDDAM and S. TOSTO, in Proceedings of the Sixth International Conference on Intergranular and Interphase Boundaries in Materials, Tessaloniki, June 1992, edited by P. Komminou and A. Rocher. (Trans. Tech., Aedemansderf, Switzerland, 1993).
7. P. VANHILLE, S. TOSTO, J. M. PELLETIER, A. ISSA, A. B. VANNES and B. CRIQUI, *Surf. Coat. Technol.* **50** (1992) 295 and 303.
8. F. GAUZZI, G. PRINCIPI and S. TOSTO, in Proceedings of the Second European Conference on Advanced Materials and Processes, Cambridge, July 1991, edited by T. W. Clyne and P. J. Withers. (The Institute of Materials, London, 1991).
9. C. VIGNAUD, L. BEAUNIER, A. LA BARBERA, A. MIGNONE and S. TOSTO, in "Duplex Stainless Steels '91", Vol. 1, edited by C. S. Bernhardsson, Beaune October 1991.
10. A. LA BARBERA, A. MIGNONE, S. TOSTO and C. VIGNAUD, *Surf. Coat. Technol.* **46** (1991) 317 and 329.
11. *Idem., J. Mater. Sci. Lett.* **10** (1991) 1370 and 1373.
12. R. KUPFER, B. BIERMANN and H. W. BERGMANN, in Proceedings of ECLAT '90, edited by H. W. Bergmann and R. Kupfer. AWT, Erlangen, September 1990. (Sprechsaal, Coburg, Germany, 1991).
13. J. PHILIBERT, "Diffusion et transport de matiere dans les solides" (Editions de Physique, Les Ulis Cedex, 1990).
14. R. W. CAHN and P. HAASEN, "Physical metallurgy" (North Holland, Amsterdam, 1983).

*Received 30 March*
*and accepted 3 August 1993*